

## Original Article

Effects of S906T polymorphism on the severity of a novel borderline mutation I692M in Na<sub>v</sub>1.4 cause periodic paralysis

Fan C., Mao N., Lehmann-Horn F., Bürmann J., Jurkat-Rott K. Effects of S906T polymorphism on the severity of a novel borderline mutation I692M in Na<sub>v</sub>1.4 cause periodic paralysis.

*Clin Genet* 2017; 91: 859–867. © John Wiley & Sons A/S. Published by John Wiley & Sons Ltd, 2016

Hyperkalemic periodic paralysis (HyperPP) is a dominantly inherited muscle disease caused by mutations in *SCN4A* gene encoding skeletal muscle voltage gated Na<sub>v</sub>1.4 channels. We identified a novel Na<sub>v</sub>1.4 mutation I692M in 14 families out of the 104 genetically identified HyperPP families in the Neuromuscular Centre Ulm and is therefore as frequent as I693T (13 families out of 14 HyperPP families) in Germany. Surprisingly, in 13 families, a known polymorphism S906T was also present. It was on the affected allele in at least 10 families compatible with a possible founder effect in central Europe. All affected members suffered from episodic weakness; myotonia was also common. Compared with I692M patients, I692M-S906T patients had longer weakness episodes, more affected muscles, CK elevation and presence of permanent weakness.

Electrophysiological investigation showed that both mutants had incomplete slow inactivation and a hyperpolarizing shift of activation which contribute to membrane depolarization and weakness. Additionally, I692M-S906T significantly enhanced close-state fast inactivation compared with I692M alone, suggesting a higher proportion of inactivated I692M-S906T channels upon membrane depolarization which may facilitate the initiation of weakness episodes and therefore clinical manifestation. Our results suggest that polymorphism S906T has effects on the clinical phenotypic and electrophysiological severity of a novel borderline Na<sub>v</sub>1.4 mutation I692M, making the borderline mutation fully penetrant.

**Conflict of interest**

The authors declare that they have no conflict of interest.

C. Fan<sup>a</sup>, N. Mao<sup>a,b</sup>,  
F. Lehmann-Horn<sup>a</sup>, J.  
Bürmann<sup>c</sup> and K. Jurkat-Rott<sup>d</sup>

<sup>a</sup>Division of Neurophysiology, Ulm University, Ulm, Germany, <sup>b</sup>Human Oncology & Pathogenesis Program, Memorial Sloan Kettering Cancer Center, New York, NY, USA, <sup>c</sup>Department of Neurology, University Hospital of the Saarland, Homburg, Germany, and <sup>d</sup>Dept. of Neurosurgery, Ulm University, Albert-Einstein-Allee 23, 89081 Ulm, Germany

Key words: founder effect – hyperkalemic periodic paralysis – Na<sub>v</sub>1.4 – novel borderline mutation

Corresponding author: Karin Jurkat-Rott, Dept. of Neurosurgery, Albert-Einstein-Allee 23, 89081 Ulm, Germany. Tel.: +498221/96-2164; fax: +498221/96-2158; e-mail: Karin.jurkat-rott@uni-ulm.de

Received 2 August 2016, revised and accepted for publication 30 September 2016

Hyperkalemic periodic paralysis (HyperPP) is a dominantly inherited muscle disease characterized by episodes of flaccid weakness when extracellular potassium increases (1). The prevalence of HyperPP is approximately 1/200,000, and its penetrance is high (>90%) (2). Triggers of HyperPP include potassium-rich food, rest after exercise and fasting. Clinically, HyperPP can present as isolated episodic weakness or be associated with clinical or EMG myotonia (1, 3).

Until now, more than 10 mutations in *SCN4A* gene encoding Na<sub>v</sub>1.4 channels have been identified to cause HyperPP (4–6). The coding region of *SCN4A* consists of 24 exons and 23 introns (7). Codon changes in exons 9, 13, 19, 23 and 24 have been reported to cause HyperPP. Four pathogenic substitutions have been identified in exon 13, leading to mutations including T704M, I693T and L689I/V which account for more than 2/3 of all HyperPP patients (1, 4, 8).

HyperPP mutations either affect the intracellular loops or the transmembrane segments of Na<sub>v</sub>1.4 channels involved in inactivation (6, 9). Fast and slow inactivation of Na<sub>v</sub>1.4 channels work in concert to regulate the fraction of available sodium channels and control the membrane excitability of skeletal muscle cells. As two independent processes, fast inactivation occurs within milliseconds, terminating the generation of action potentials, while slow inactivation happens in seconds to minutes, governing the availability of excitable sodium channels (10, 11). Sustained inward sodium current due to disrupted fast inactivation with re-opening persistent current is a common feature for several HyperPP mutations (5, 12). The persistent inward current may also be generated by an increased window current created by shifting of voltage-dependence of either activation or both activation and inactivation (12–14). When the membrane is slightly depolarized by elevated extracellular potassium brought about by ingestion or exercise, such persistent current could further depolarize the membrane and facilitate the generation of repeated action potentials, leading to myotonia (4, 9). On the other hand, the depolarization drives potassium ions out of the cell causing higher extracellular potassium and further membrane depolarization (4, 6, 8, 9). When the membrane potential depolarizes beyond the threshold it inactivates Na<sub>v</sub>1.4 channels leading to muscle paralysis. (4, 9). Defects in channel slow inactivation also contribute to clinical weakness. Over seconds to minutes, slow inactivation will occur due to the sustained depolarization. Sodium channels will enter into slow inactivated state, decreased the number of excitable channels and sodium influx, leading to repolarization of membrane potentials (15, 16). Incomplete slow inactivation could lead to persistent sodium current which inactivates Na<sub>v</sub>1.4 channels, such as HyperPP mutations of L689I, I693T, T704M and M1592V (14, 17, 18).

The polymorphism S906T, encoded by exon 14 and located in II–III loop of Na<sub>v</sub>1.4 channel has been described in 4% healthy German population and in 1.8% worldwide controls (19) (<http://exac.broadinstitute.org>). Electrophysiological characterization of S906T revealed no effects on fast gating process of Na<sub>v</sub>1.4 channels, but slowed entry into and recovery from slow inactivation (19).

In the present study, we identified a C2076G base change in exon 13 leading to a novel mutation I692M in the Na<sub>v</sub>1.4 channel. The mutation was found in 14 families, 13 of which had another G2717C base change in exon 14 predicting the known polymorphism S906T. It was on the affected allele in at least 10 families compatible with a possible founder effect in central Europe. Clinical analysis and electrophysiological investigations showed that S906T exerted an influence on the severity of both clinical phenotypes and gating change of the borderline I692M mutation.

## Materials and methods

Genetics and phenotype

Fourteen HyperPP families were enrolled into this study for mutation screening and clinical analysis. Informed

consent was obtained from all participants, and all procedures were approved by the Ethics Committee of Ulm University and were in accordance with the Declaration of Helsinki. Direct sequencing of all SCN4A exons was performed using the Sanger method.

## Electrophysiological studies

The human Na<sub>v</sub>1.4  $\alpha$  subunit sub-cloned to the pEGFP vector was used for site-directed mutagenesis of both I692M and I692M-S906T mutations. Whole-cell patch clamp recordings were performed 24 h after transient transfection of SCN4A in human tsA201 cells using the jetPEI kit. The pipette resistance was around 1.5 M $\Omega$  after filling with internal solution containing (in mM): NaCl 35, CsF 105, EGTA 10, HEPES 10. The external solution contained (in mM) NaCl 150, KCl 2, CaCl<sub>2</sub> 1.5, MgCl<sub>2</sub> 1, HEPES 10. pH was adjusted to 7.4 and osmolarity to approximately 300 mOsm. Before data acquisition, cells were allowed to stabilize for 10 min after establishment of the whole-cell configuration. Sodium currents were recorded at room temperature (21–23°C) with 4/P leak subtraction after partial series resistance compensation (~85%) using an Axopatch 200B amplifier (Molecular Devices, Union City, CA, USA). Data were filtered at 10 kHz and sampled at 50 kHz.

## Data analysis

The steady-state activation was determined by fitting conductance–voltage relation with the equation:  $G/G_{\max} = A/(1 + \exp((V - V_{0.5})/k))$  with  $A$  the fraction of activated channels,  $V_{0.5}$  the potential for half-maximal current,  $V$  the test potentials, and  $k$  the slope factor. Steady-state inactivation curves were evaluated by fitting the data to the equation:  $I/I_{\max} = A/(1 + \exp((V_{0.5} - V)/k)) + C$  with  $V$  representing the pre-pulse potential,  $V_{0.5}$  the potential at which half of the channels are inactivated,  $C$  the fraction of non-inactivated channels, and  $k$  the slope factor. Time constants of fast inactivation were obtained by fitting a single exponential function to the current decay:  $t = A \cdot \exp(-t/\tau) + C$  with  $t$  being the time,  $A$  the fraction of channels inactivating with time constant  $\tau$ , and  $C$  the asymptote. The recovery from inactivation was analyzed by fitting the data with the equation:  $I/I_{\max} = A \cdot (1 - \exp(-(t_0 - t)/\tau))$  with  $\tau$  denoting the time constant, and  $A$  representing the fractional amplitude. The recovery from slow inactivation was analyzed by fitting the data with a double exponential function:  $I/I_{\max} = A_{\text{fast}} \cdot (1 - \exp(-t/\tau_{\text{fast}})) + A_{\text{slow}} \cdot (1 - \exp(-t/\tau_{\text{slow}})) + C$ , with  $\tau_{\text{fast}}$  and  $\tau_{\text{slow}}$  denoting a fast and a slow time constant,  $A_{\text{fast}}$  and  $A_{\text{slow}}$  representing the two fractional amplitudes, and  $C$  the level of non-inactivating sodium current. Entry into closed-state inactivation and entry into slow inactivation were obtained by fitting a single exponential decay equation.

Data were analyzed by a combination of pClamp (Molecular Devices), Excel (Microsoft), SPSS (IBM) and ORIGIN (Microcal software). Data are presented

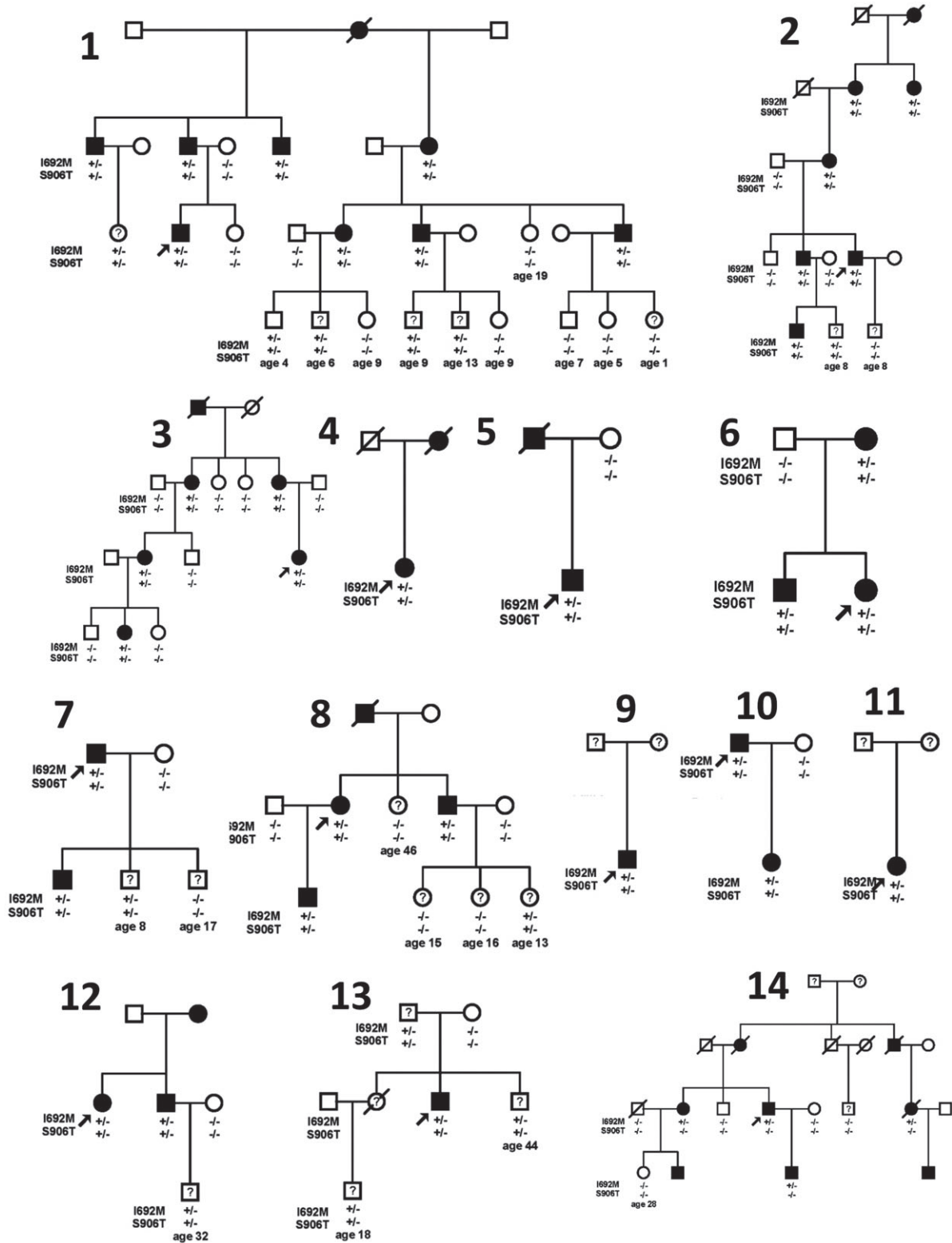


Fig. 1. Pedigrees of 14 HyperPP families with mutation status of I692M or S906T. Affected individuals are shown as solid symbols. Squares represent males and circles represent females. Question marks indicate that no clinical information was available to determine clinical status at the age indicated. In families 1–13, all patients (affected individuals) have both I692M and S906T. Note that there is at least one unaffected parent carrying neither of the variants in 10 of the families (numbers 1–3, 5–8, 10, 12–13) proving that both variants come from the affected parent and are therefore on the same allele. Family 14 is the only family having I692M without S906T.

Table 1. Clinical features of HyperPP families<sup>a</sup>

	I692M-S906T	I692M
Number of families/individuals	13/29	1/2
Clinical features		
Onset age	14.6	14
Frequency: daily/weekly/monthly/yearly or less	23%/55%/14%/8%	50%/0/50%/0
Duration: minutes/hours/days	14%/55%/32%	100%/0/0
Myotonia	61%	50%
Permanent weakness	28%	0
Average serum CK (U/l/% <sup>b</sup> )	795.25%/28%	187.50%/100%
Muscles affected		
Proximal/distal	87%/59%	100%/100%
Face/neck/larynx	86%/34%/28%	0/0/0
Trunc/abdominal	4%/4%	0/0
Triggers		
Fasting/sport/rest after exercise	33%/46%/42%	100%/50%/100%
Stress/eating/cold/K <sup>+</sup>	38%/21%/8%/8%	50%/0/0/0
Medication		
Hydrochlorothiazide	41%	100%
Acetazolamide	10%	100%
Glucose/flupirtin	10%/4%	0/50%
Salbutamol/potassium	17%/4%	0/0

<sup>a</sup>Only patients with both detailed clinical data and clear genetic diagnosis have been included in the analysis in Table 1.

<sup>b</sup>Indicates percentage of the 29 patients with serum CK data.

as mean  $\pm$  standard error of the mean (SEM). Student's *t*-test were applied for statistical evaluation with significance levels set to  $p < 0.05$ ,  $p < 0.01$  and  $p < 0.001$ .

## Results

### Genetics and phenotype

Sanger sequencing of all exons of SCN4A revealed that all 14 HyperPP families harbor a heterozygous G to C substitution at nucleotide 2076 in exon 13, corresponding to an I692M mutation in the S4-S5 linker of domain II in Na<sub>v</sub>1.4 channels (Fig. 1). This variant has not been reported in 60706 alleles included in the ExAC browser, however, a similar substitution, I692T, was found in 1 of those 60,706 controls (<http://exac.broadinstitute.org>). Thirteen out of the 14 HyperPP families also had a G2717C base exchange in exon 14, predicting the known polymorphism S906T, in all affected individuals (Fig. 1). In the three of these families, the parents of the probands were unavailable for testing. However, in the other 10 of these families, at least one unaffected parent in one generation did not carry either variant proving that the two variants, coding for I692M and S906T, were both inherited from the affected parent (Fig. 1). This means that the two variants were on the same allele.

In all patients, episodic paralysis was reported with onset at approximately 14 years old. Myotonia was also a common clinical sign, affecting about 61% of all patients. Frequency of episodic weakness varied from daily to monthly. Tendentially, paralytic attacks lasted longer in patients with I692M-S906T than patients with the single I692M mutation (Table 1).

During attacks, mostly extremity muscles were affected. Facial, laryngeal, and neck muscles were involved in the patients with I692M-S906T mutation but not in patients with I692M mutation. Typical triggers of paralytic attacks were fasting, sports, longer rest, eating and stress. About 28% of patients with I692M-S906T showed permanent muscular weakness whereas no permanent weakness was present in patients with only I692M mutation. Also, patients with I692M-S906T showed elevated CK (averaged value of 795.25 U/l). Summarizing it up, the shorter the attack duration, the less affected muscles, the absence of permanent muscular weakness and the absence of CK elevation may indicate that patients carrying only I692M mutation are clinically less affected than patients with I692M-S906T (Table 1).

As a prophylactic treatment of paralytic episodes, hydrochlorothiazide had a beneficial effect on nine of 11 patients with I692M-S906T mutation which was applied. Acetazolamide was also able to reduce the attack frequency in two of three patients with I692M-S906T. During an acute episode, glucose intake or inhaled salbutamol may be beneficial. Due to the small number of patients, these therapeutic results should be interpreted cautiously (Table 1) even though the response to therapy for our families is similar to previously described HyperPP patients (1, 4, 6). The prophylactically taken diuretics, hydrochlorothiazide and acetazolamide, both reduce serum potassium, an important trigger for weakness (1, 4, 6). They also increase acidification and thereby increase muscle excitability and muscle dynamics, especially if the muscles are pre-depolarized due to high potassium (20, 21). During acute episodes of weakness, glucose intake leads to increased Na<sup>+</sup>/K<sup>+</sup>-ATPase activity with increased potassium uptake reducing serum potassium (22). Likewise, inhaled salbutamol is known to decrease serum potassium in emergencies by the same mechanism (23).

### Electrophysiology

Heterologous expression of wild type (WT), I692M and I692M-S906T channels produced typical inward sodium currents (Fig. 2a). The corresponding conductance–voltage relationship revealed an almost  $-4$  mV shift for I692M compared with WT which did not reach significance levels. And there was a significant  $-4$  mV shift for I692M-S906T compared with the I692M. S906T enhanced the hyperpolarization shift in voltage-dependence of activation of I692M (Fig. 2b and its inset, Table 2). The hyperpolarization shift of activation curves is reminiscent of the negative shifting of activation curves reported for the known HyperPP mutations L689I and I693T which are also located in

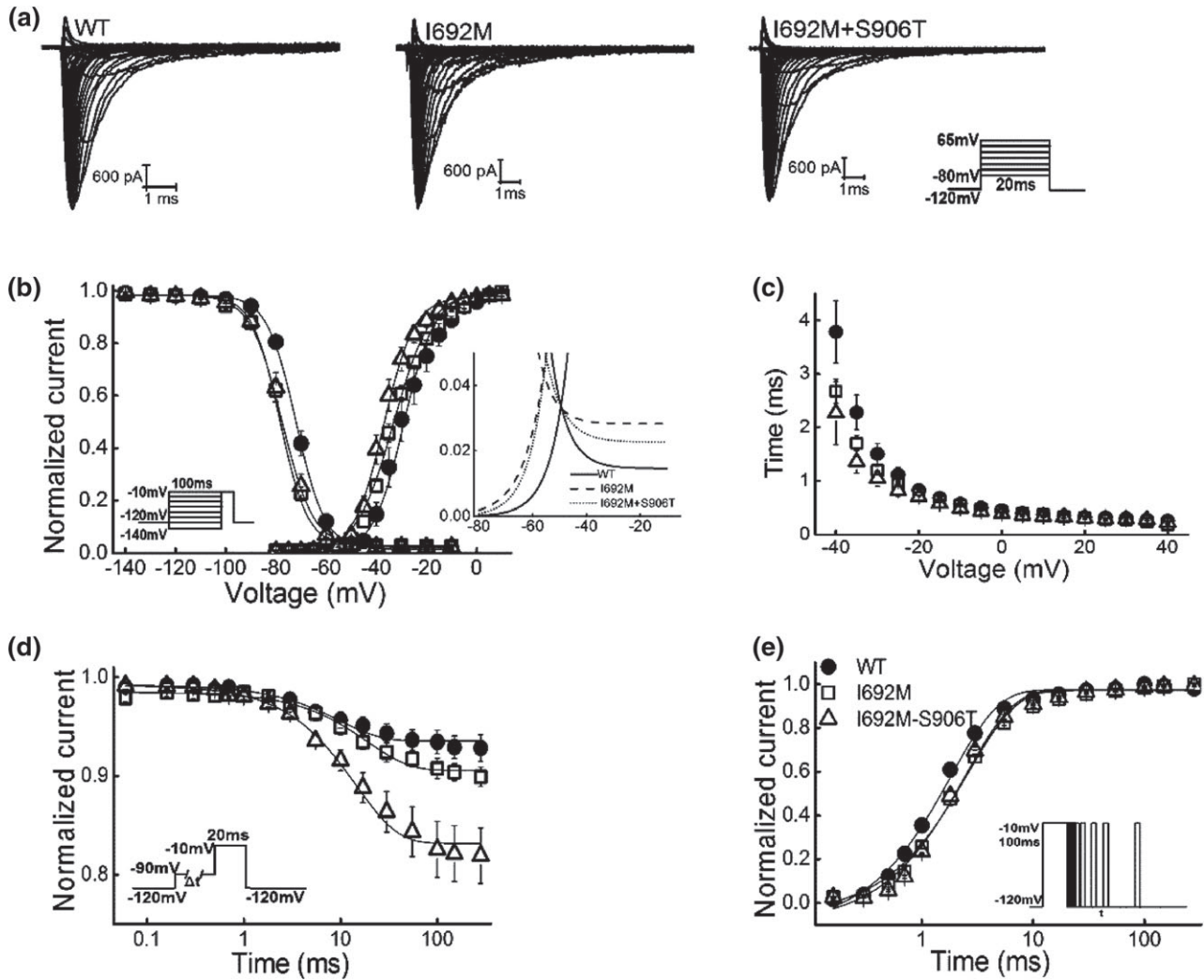


**Fig. 2.** Functional characteristics of WT (filled circles), mutant I692M (open squares) and I692M+S906T (open triangles) channels expressed in tsA201 cells. (a) Typical whole-cell currents responding to the activation protocols shown in inset. (b) Steady-state fast inactivation curves and conductance–voltage curves. Inactivation curves were determined from a holding potential of  $-120$  mV using a series of 100 ms pre-pulses to potentials between  $-140$  and  $-10$  mV in 10 mV steps followed by a  $-10$  mV test pulse (WT:  $n = 10$ , I692M:  $n = 10$  and I692M+S906T:  $n = 11$ ). Activation curves were elicited from a holding potential of  $-120$  mV by voltage steps between  $-80$  and  $+65$  mV in 5 mV intervals for 20 ms pulse (WT:  $n = 10$ , I692M:  $n = 10$  and I692M+S906T:  $n = 11$ ). Enlarged window current was shown in inset. (c) Voltage-dependence of time constants of fast inactivation of WT and mutant channels (WT:  $n = 10$ , I692M:  $n = 10$  and I692M+S906T:  $n = 11$ ). (d) Time course of closed-state inactivation for durations from 0.06 to 280 ms at  $-90$  mV from a holding potential of  $-120$  mV whereby a test pulse to  $-10$  mV determined the fraction of non-inactivated channels (WT:  $n = 12$ , I692M:  $n = 11$  and I692M+S906T:  $n = 11$ ) (e) Recovery from fast inactivation with a two-pulse protocol: a 100 ms-lasting depolarization pre-pulse to  $-10$  mV was used to inactivate sodium channels, a second  $-10$  mV test pulse followed after an increasing interval from 0.16 to 280 ms from a holding potential of  $-120$  mV (WT:  $n = 9$ , I692M:  $n = 10$  and I692M+S906T:  $n = 14$ ). Protocols are shown in insets. Data are shown as means  $\pm$  SEM. Lines are fits to corresponding equations. Fitting parameters are listed in Table 2.

S4-S5 linker of domain II (14, 24). Also such shift of activation curves leads to increased peak window current with the values of 3.9% and 3.5% of the peak central current compared with 2.7% for the WT, and a hyperpolarization shift for voltage range of the peak window current:  $-54.7$  mV and  $-54.4$  mV for I692M and I692M-S906T compared with  $-48.8$  mV for WT (Fig. 2b inset and Table 2). This is in agreement with the persistent sodium currents recorded at voltage range between  $-75$  and  $-40$  mV in Hyperpp muscle fibers leading to depolarized membrane potentials with increased extracellular potassium (25).

The time constant of fast inactivation which was fitted to a single exponential function revealed no difference for both I692M and I692M-S906T than the WT over the range of  $-40$  to  $40$  mV (Fig. 2c). Even though persistent current is a common feature for HyperPP mutations, neither I692M nor I692M-S906T produced such additional persistent current after both 20 ms (Fig. 2a) and 100 ms (data not shown) depolarization which is in agreement with the undistinguishable time constant of fast inactivation between the two mutants and WT.

However, I692M and I692M-S906T both showed around  $-5$  mV hyperpolarization shift in voltage gated

Table 2. Gating parameters of wild type (WT) and both mutations

Parameters	WT	I692M	I692M-S906T
Activation	$n = 10$	$n = 10$	$n = 11$
$V_{0.5}$ (mV)	$-28.82 \pm 2.36$	$-33.02 \pm 0.94$	$-36.93 \pm 1.38^{****}$
$K$	$-5.57 \pm 0.48$	$-6.83 \pm 0.36$	$-5.31 \pm 0.44^{****}$
Fast inactivation	$n = 10$	$n = 10$	$n = 11$
$V_{0.5}$ (mV)	$-71.65 \pm 1.15$	$-77.40 \pm 1.06^{**}$	$-76.70 \pm 1.44$
$k$	$-5.23 \pm 0.17$	$-5.28 \pm 0.12$	$-5.26 \pm 0.09$
Window current	$n = 10$	$n = 10$	$n = 11$
Peak window current (% of peak)	$2.7\% \pm 0.25\%$	$3.9\% \pm 0.23\%^{**}$	$3.5\% \pm 0.27\%$
Voltage of peak window current	$-48.75 \pm 1.20$	$-54.71 \pm 0.9^{**}$	$-54.35 \pm 0.27$
Entry into closed inactivation	$n = 12$	$n = 11$	$n = 11$
$\tau$ (ms)	$14.79 \pm 3.44$	$22.63 \pm 5.80$	$19.24 \pm 3.32$
$A$	$0.06 \pm 0.01$	$0.08 \pm 0.01$	$0.17 \pm 0.03^{****}$
Recovery from fast inactivation	$n = 9$	$n = 10$	$n = 14$
$\tau$ (ms)	$1.81 \pm 0.16$	$2.60 \pm 0.24^*$	$2.46 \pm 0.12$
Entry into slow inactivation	$n = 5$	$n = 6$	$n = 7$
$\tau$ (ms)	$2355.6 \pm 344.7$	$1566.7 \pm 223.2$	$968.71 \pm 92.3^{****}$
$c$	$0.11 \pm 0.02$	$0.28 \pm 0.01^{***}$	$0.32 \pm 0.03$
Slow inactivation	$n = 6$	$n = 8$	$n = 9$
$V_{0.5}$ (mV)	$-58.07 \pm 3.78$	$-49.87 \pm 2.77$	$-52.59 \pm 2.86$
$k$	$-12.50 \pm 0.96$	$-13.86 \pm 0.95$	$-14.90 \pm 1.50$
$c$	$0.11 \pm 0.02$	$0.22 \pm 0.04^*$	$0.26 \pm 0.03$
Recovery from slow inactivation	$n = 8$	$n = 6$	$n = 6$
$\tau_{\text{fast}}$ (ms)	$96.36 \pm 25.22$	$25.22 \pm 6.34^*$	$26.73 \pm 3.7$
$\tau_{\text{slow}}$ (ms)	$1100.98 \pm 306.64$	$350.0 \pm 53.0^*$	$309.49 \pm 44.0$

Significance levels set to \* $p < 0.05$ , \*\* $p < 0.01$  and \*\*\* $p < 0.001$  for I692M vs WT, and \*\*\*\* $p < 0.05$  for I692M-S906T vs I692M.

steady-state fast inactivation (Fig. 2b, Table 2). Additionally, mutation I692M-S906T exhibited enhanced closed-state fast inactivation, leading to more inactivated channels compared with the WT and I692M at the membrane potential of  $-90$  mV (Fig. 2d). After 280 ms, I692M-S906T showed 17% inactivated channels compared with 6% and 8% for the WT and I692M, respectively (Fig. 2d, Table 2), and S906T further increased I692M effects on the enhanced entry into closed state. Alterations in fast inactivation and the observed slower recovery from fast inactivation for both I692M and I692M-S906T mutations (Fig. 2e) were in agreement with the hyperpolarization of steady-state inactivation, which was unlike the mutations L689I and I693T (14, 24). This result indicates that S4-S5 linker of domain II is involved in the fast inactivation process of  $\text{Na}_v1.4$  channels. In agreement with the alterations of fast inactivation and recovery, stimulations of repetitive depolarized pulses at different frequencies and from different holding potentials showed enhanced use-dependent block for both I692M and I692M-S906T (Fig. 3). S906T increased this effect and displayed around 18% more use-dependent reduction compared to the WT with the simulation frequency of 125 Hz from a holding potential of  $-90$  mV.

Disruption of slow inactivation, another common feature among HyperPP mutations, was present in both I692M and I692M-S906T. Although I692M-S906T showed a significant faster entry into slow inactivation state (Table 2), both mutants showed incomplete slow inactivation, leading to 28–32% of non-inactivated channels compared with 11% for WT (Fig. 4a, Table 2).

Boltzmann fitting parameters of slow inactivation of I692M and I692M-S906T did not differ from WT, however, at potentials more positive than  $-60$  mV, both mutants showed more available channels than the WT after a 30s depolarization pulse. For example, I692M and I692M-S906T showed 22–26% non-inactivated sodium channels compared with 11% for WT (Fig. 4b, Table 2). The incomplete slow inactivation exhibited by I692M and I692M-S906T mutations is similar to the impaired slow inactivation caused by the known HyperPP mutations L689I, I693T, T704M and M1592V whose predominant symptom is episodic weakness (12–14, 17, 18). Additionally, all three channels were recovered in a bi-exponential way from slow inactivation. I692M and I692M-S906T showed significant faster recovery rates compared with the WT, with decreased fast and slow time constants, leading to significantly more available sodium channels (Fig. 4c, Table 2). S906T increased I692M effects of reduced entry into slow inactivation, enhanced fraction of non-inactivated sodium channels and faster recovery from slow inactivation.

Altogether, I692M and I692M-S906T showed (i) incomplete slow inactivation, (ii) hyperpolarization shift in voltage gated activation and therefore a negative shift and increased amplitude of window current. Additionally, I692M-S906T significantly enhanced closed-state fast inactivation compared with I692M alone.

## Discussion

The I692M mutation accounted for 13.5% of the 104 genetically clarified HyperPP families of the

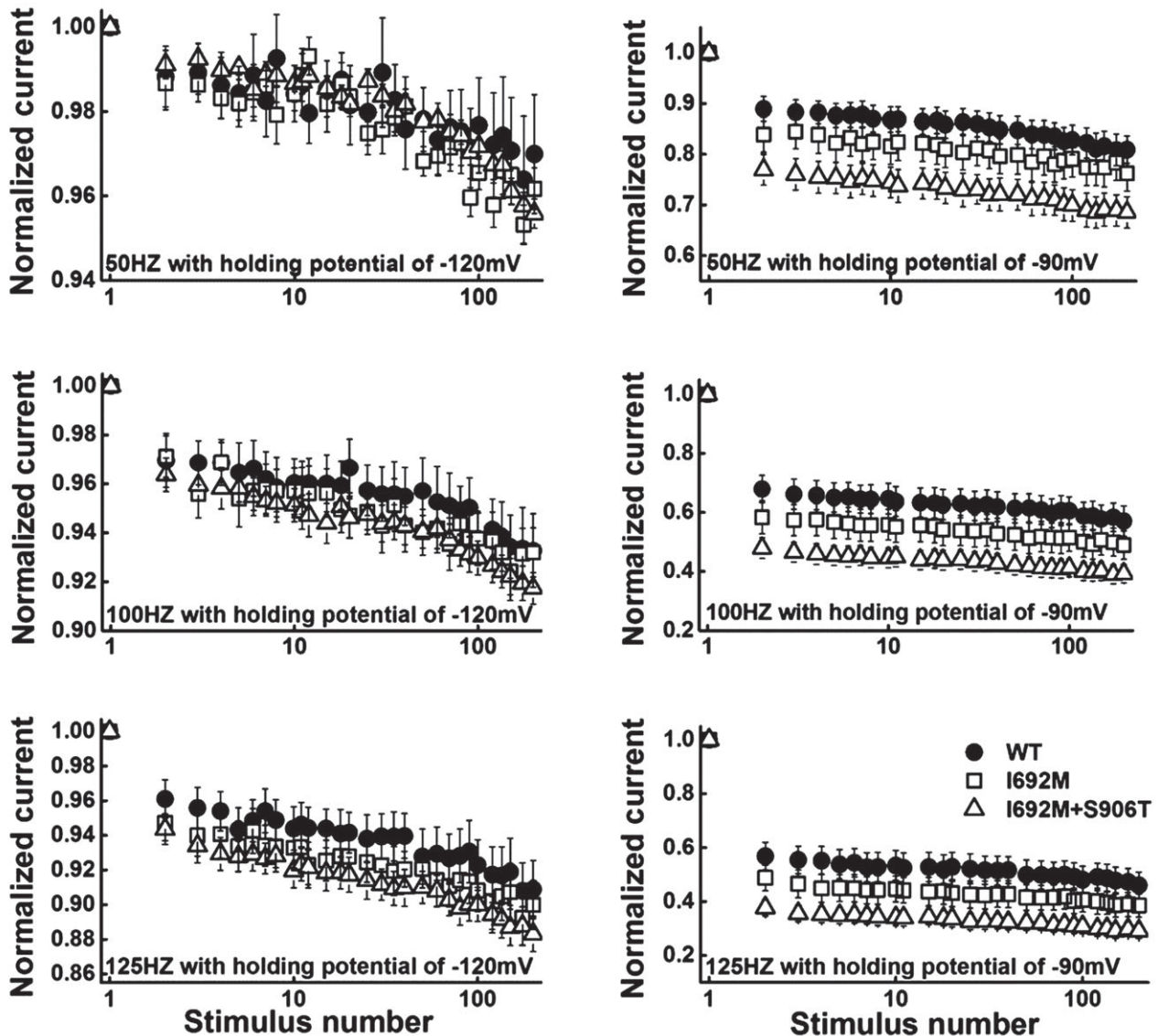
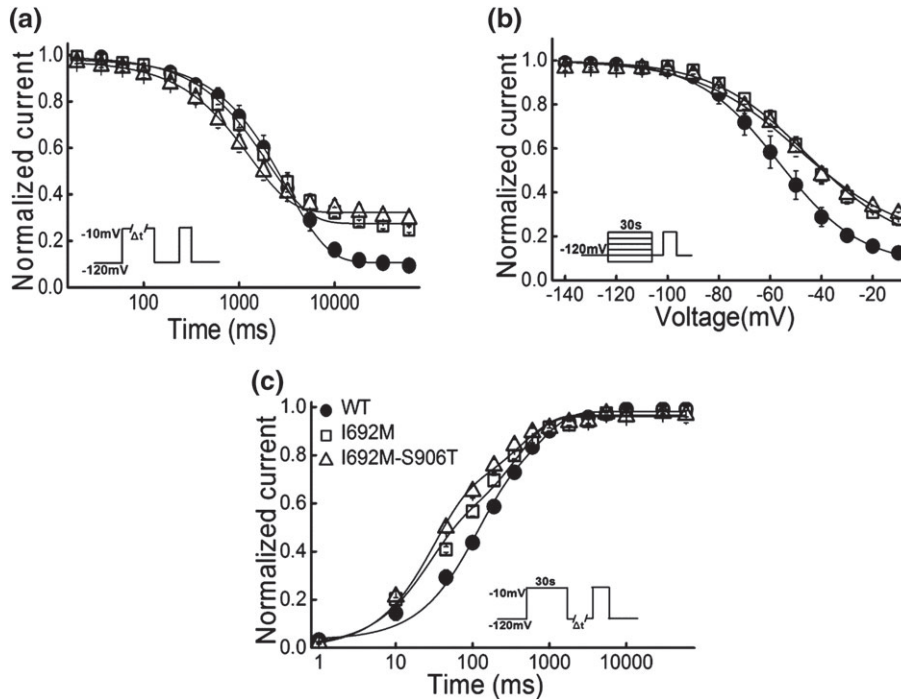


Fig. 3. Use dependence of WT (filled circles), mutant I692M (open circles) and I692M + S906T (open triangles) channels. Currents were elicited by 200 consecutive trains of 2 ms-long depolarizing pulses to  $-10$  mV from different holding potentials [ $-120$  mV (left graphs) and  $-90$  mV (right graphs)] at different frequencies [50 Hz (top graphs), 100 Hz (middle graphs) and 125 Hz (bottom graphs)]. Each trace was normalized to the initial transient peak sodium current. Necessary but not all data points are shown for clarity. Data are shown as means  $\pm$  SEM.

Neuromuscular Centre Ulm and is as frequent as I693T in Germany (in 13 of 104 families). The patients carrying I692M-S906T mutation showed longer weakness episodes, more muscles affected, CK elevation and presence of permanent weakness indicating that S906T exacerbates the phenotype. Such a mild phenotype might explain why this novel I692M mutation was not identified before because it should have been found since exon 13 is always sequenced for HyperPP diagnosis as this exon accounts for 2/3 of causative mutations (1, 4, 8).

If the G2717C base change coding for S906T may be considered as a genetic marker, then the co-occurrence with G2076C coding for I692M may either be coincidental or the result of a founder effect. Taking just the 10 families in which the presence of both variants on

the same allele is proven by the mode of inheritance, the probability of the co-occurrence of the two variants being coincidental (independent), is  $1:2^{10} = 0.1\%$ . In a statistical test, a likelihood of error (type 1 error) of anything less than 5% would lead to rejection of the null hypothesis. Therefore, statistically, it is reasonable to assume that the allele in the 10 families is identical (founder effect), namely with a probability of 99.9%. When taking into account the allele frequencies of the variants, an even lower likelihood of error is reached when considering that the polymorphism coding for S906T has been described in only 4% of the German population (19), that G2076C coding for I692M is present in 14 of the 104 genetically clarified HyperPP families of the Ulm Neuromuscular Centre, and that the disease has a prevalence of, at most, 1:100,000 (1). Then, the



**Fig. 4.** Slow inactivation properties of WT (filled circles), mutant I692M (open circles) and I692M + S906T (open triangles) channels. (a) Entry into slow inactivation was elicited from a holding potential of  $-120$  mV by a depolarizing pulse to  $-10$  mV for an increasing time period (0.02–60 s). An interval of 50 ms at  $-120$  mV followed to recover the fast inactivated but not slow inactivated channels. Then the fraction of slow inactivated channels was determined by the following 20 ms test pulse to  $-10$  mV (WT:  $n = 5$ , I692M:  $n = 6$  and I692M + S906T:  $n = 7$ ). (b) Steady-state slow inactivation was determined by a 30 s conditioning pulse between  $-140$  and  $-10$  mV, followed by a 50 ms recovery period at  $-120$  mV prior to the  $-10$  mV test pulse (WT:  $n = 6$ , I692M:  $n = 8$  and I692M + S906T:  $n = 9$ ). (c) Recovery from slow inactivation was measured by a 30 s depolarizing pulse to  $-10$  mV followed by increasing recovery duration (from 0.001–60 s) from holding potential of  $-120$  mV. The test pulse to  $-10$  mV was then employed to record the recovered sodium currents (WT:  $n = 8$ , I692M:  $n = 6$  and I692M + S906T:  $n = 6$ ). For all slow kinetics investigation cells were held at  $-120$  mV between trials for 30 s to allow the recovery from slow inactivation. Protocols are shown in insets. Data are shown as means  $\pm$  SEM. Lines are fits to corresponding equations. Fitting parameters are listed in Table 2.

probability of a single co-occurrence on the same allele is  $0.04 \times 14/104 \times 1/100,000 = 5.4 \times 10^{-8}$ ; for 10 families, it would be  $2 \times 10^{-73}$ . Therefore, in the 10 families for which we had both parents in at least one generation, the most likely explanation for the two variants to be on the same allele would be a founder effect. The localization of the variants in adjacent exons strengthens the idea that they have not been separated by crossing-over.

Typical for other HyperPP mutations, when the membrane is slightly pre-depolarized by hyperkalemia, increased window current or persistent current further depolarizes membrane potentials and leads to inactivation of both normal and mutant sodium channels (9). Also, incomplete slow inactivation leading to more available channels and additional depolarizing sodium conductance causes muscle weakness by membrane depolarization in HyperPP (11, 15, 16). I692M showed both of these typical HyperPP mechanisms, namely the hyperpolarizing-shifted and increased amplitude of window current and incomplete slow inactivation. Therefore we consider I692M to be a HyperPP mutation.

For HyperPP mutations, usually the disease-causing persistent current is around 5–10% of the peak current (12, 26), while I692M and I692M-S906T only showed a maximal window current less than 4% of the peak current, which is in agreement with the corresponding

milder phenotypes. Our patients had episodes of shorter duration: 69% of I692M-S906T patients had attacks lasting minutes to hours, while patients of I692M only reported attacks lasting a few minutes. In contrast, in the literature 35% of 137 HyperPP patients had attacks with duration lasting minutes to hours; the rest had longer attacks (3). Likewise, our patients had less permanent weakness: 28% of I692M-S906T patients and none of I692M patients reported permanent weakness compared with 35.6% of 137 HyperPP patients reported permanent weakness in the literature (3).

The allelic S906T polymorphism significantly enhanced closed-state fast inactivation compared with I692M alone, suggesting that a higher proportion of I692M-S906T channels will be inactivated upon membrane depolarization which may facilitate the initiation of weakness episodes, thereby contributing to clinical disease manifestation (27). Therefore, I692M-S906T patients may consult a doctor earlier than I692M patients and are subject to genetic diagnosis.

The structural basis for the observed functional effects is somewhat speculative. The S4-S5 loop of domain II which connects the voltage sensing S4 segment to the pore-forming S5-S6 segments of channel domain II, contains I692M as well as the known HyperPP mutations, I693T and L689I. Therefore, both by previous

reports (14, 24) as well as by our results here, the S4–S5 loop understandably affects gating and contributes to both activation and inactivation. In contrast, not much about the functional significance of the interlinker connecting domains II and III in which S906T is located is known. In neuronal channels, the II–III linker contains signals for cell compartmentalization, i.e. clustering of sodium channels in specific areas of the axon (28); in the muscle channel, the linker is important for slow inactivation (19). Since the functional effects of the double mutation I692M-S906T do not equal to a simple addition of the gating alterations of I692M alone and S906T alone (19), some sort of mutual influence or interaction between II–III linker and IIS4-S5 loop may be assumed. This interaction may be a requirement for slow inactivation.

Taken together, this is the first report of a functional polymorphism exacerbating the phenotype of an allelic ion channelopathy with a possible founder effect in central Europe.

### Acknowledgements

We thank the funding support by non-profit Hertie-Foundation, the German Society for Muscle Disorders (DGM), and the IonNeurOnet of the German Federal Ministry of Research (BMBF). We thank Marius Kuhn for helpful discussions. We thank all the patients and relatives for their cooperation in this study.

### References

- Weber F, Jurkat-Rott K, Lehmann-Horn F. Hyperkalemic periodic paralysis. In: GeneReviews®. Seattle, WA: University of Washington, 1993.
- Lehmann-Horn F, Rudel R. Channelopathies: the nondystrophic myotonias and periodic paralyses. *Semin Pediatr Neurol* 1996; 3: 122–139.
- Charles G, Zheng C, Lehmann-Horn F, Jurkat-Rott K, Levitt J. Characterization of hyperkalemic periodic paralysis: a survey of genetically diagnosed individuals. *J Neurol* 2013; 260: 2606–2613.
- Simkin D, Bendahhou S. Skeletal muscle na channel disorders. *Front Pharmacol* 2001; 2: 63.
- Lossin C, Nam TS, Shahangian S et al. Altered fast and slow inactivation of the N440K Na<sub>v</sub>1.4 mutant in a periodic paralysis syndrome. *Neurology* 2012; 79: 1033–1040.
- Jurkat-Rott K, Holzherr B, Fauler M, Lehmann-Horn F. Sodium channelopathies of skeletal muscle result from gain or loss of function. *Pflugers Arch* 2010; 460: 239–248.
- George AJ, Iyer GS, Kleinfield R, Kallen RG, Barchi RL. Genomic organization of the human skeletal muscle sodium channel gene. *Genomics* 1993; 15: 598–606.
- Miller TM, Dias da Silva MR, Miller HA et al. Correlating phenotype and genotype in the periodic paralyses. *Neurology* 2004; 63: 1647–1655.
- Jurkat-Rott K, Lehmann-Horn F. Genotype-phenotype correlation and therapeutic rationale in hyperkalemic periodic paralysis. *Neurotherapeutics* 2007; 4: 216–224.
- Vilin YY, Ruben PC. Slow inactivation in voltage-gated sodium channels: molecular substrates and contributions to channelopathies. *Cell Biochem Biophys* 2001; 35: 171–190.
- Ruff RL. Sodium channel regulation of skeletal muscle membrane excitability. *Ann N Y Acad Sci* 1997; 835: 64–76.
- Bendahhou S, Cummins TR, Tawil R, Waxman SG, Ptacek LJ. Activation and inactivation of the voltage-gated sodium channel: role of segment S5 revealed by a novel hyperkalaemic periodic paralysis mutation. *J Neurosci* 1999; 19: 4762–4771.
- Rojas CV, Neely A, Velasco-Loyden G, Palma V, Kukuljan M. Hyperkalemic periodic paralysis M1592V mutation modifies activation in human skeletal muscle Na<sup>+</sup> channel. *Am J Physiol* 1999; 276: C259–C266.
- Bendahhou S, Cummins TR, Kula RW, Fu YH, Ptacek LJ. Impairment of slow inactivation as a common mechanism for periodic paralysis in DIIS4-S5. *Neurology* 2002; 58: 1266–1272.
- Ruff RL. Slow Na<sup>+</sup> channel inactivation must be disrupted to evoke prolonged depolarization-induced paralysis. *Biophys J* 1994; 66: 542.
- Ruff RL. Alterations of Na<sup>+</sup> channel gating in myotonia. *J Physiol* 1997; 499: 571.
- Hayward LJ, Sandoval GM, Cannon SC. Defective slow inactivation of sodium channels contributes to familial periodic paralysis. *Neurology* 1999; 52: 1447–1453.
- Cummins TR, Sigworth FJ. Impaired slow inactivation in mutant sodium channels. *Biophys J* 1996; 71: 227–236.
- Kuzmenkin A, Jurkat-Rott K, Lehmann-Horn F, Mitrovic N. Impaired slow inactivation due to a polymorphism and substitutions of Ser-906 in the II-III loop of the human Na<sub>v</sub>1.4 channel. *Pflugers Arch* 2003; 447: 71–77.
- Pedersen TH, Nielsen OB, Lamb GD, Stephenson DG. Intracellular acidosis enhances the excitability of working muscle. *Science* 2004; 305: 1144–1147.
- Overgaard K, Højfeldt GW, Nielsen OB. Effects of acidification and increased extracellular potassium on dynamic muscle contractions in isolated rat muscles. *J Physiol* 2010; 588: 5065–5076.
- Rosic NK, Standaert ML, Pollet RJ. The mechanism of insulin stimulation of (Na<sup>+</sup>,K<sup>+</sup>)-ATPase transport activity in muscle. *J Biol Chem* 1985; 260: 6206–6212.
- Maxwell AP, Linden K, O'Donnell S, Hamilton PK, McVeigh GE. Management of hyperkalaemia. *J R Coll Physicians Edinb* 2013; 43: 246–251.
- Plassart-Schiess E, Lhuillier L, George AJ, Fontaine B, Tabti N. Functional expression of the Ile693Thr Na<sup>+</sup> channel mutation associated with paramyotonia congenita in a human cell line. *J Physiol* 1998; 507: 721–727.
- Lehmann-Horn F, Küther G, Ricker K, Grafe P, Ballanyi K, Rüdell R. Adynamia episodica hereditaria with myotonia: a non-inactivating sodium current and the effect of extracellular pH. *Muscle Nerve* 1987; 10: 363–374.
- Cannon SC, Strittmatter SM. Functional expression of sodium channel mutations identified in families with periodic paralysis. *Neuron* 1993; 10: 317–326.
- Groome J, Lehmann-Horn F, Holzherr B. Open- and closed-state fast inactivation in sodium channels: differential effects of a site-3 anemone toxin. *Channels (Austin)* 2011; 5: 65–78.
- Garrido JJ, Fernandes F, Moussif A, Fache MP, Giraud P, Dargent B. Dynamic compartmentalization of the voltage-gated sodium channels in axons. *Biol Cell* 2003; 95: 437–445.